

Science

 AAAS

**Surface-Modified Carbon Nanotubes Catalyze
Oxidative Dehydrogenation of n-Butane**

Jian Zhang, *et al.*

Science **322**, 73 (2008);

DOI: 10.1126/science.1161916

**The following resources related to this article are available online at
www.sciencemag.org (this information is current as of October 3, 2008):**

Updated information and services, including high-resolution figures, can be found in the online version of this article at:

<http://www.sciencemag.org/cgi/content/full/322/5898/73>

Supporting Online Material can be found at:

<http://www.sciencemag.org/cgi/content/full/322/5898/73/DC1>

This article appears in the following **subject collections**:

Chemistry

<http://www.sciencemag.org/cgi/collection/chemistry>

Information about obtaining **reprints** of this article or about obtaining **permission to reproduce this article** in whole or in part can be found at:

<http://www.sciencemag.org/about/permissions.dtl>

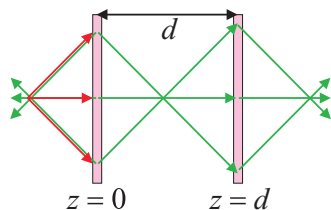


Fig. 3. Two thin sheets of time-reversing material produce a focusing effect very similar to a negatively refracting lens. The system is capable of subwavelength resolution.

Unlike the perfect lens based on negative refraction (13), loss is not an issue in this instance because the fields are translated through loss-less vacuum. The issue here is whether a time-reversing sheet can be found sufficiently powerful to give the resolution, Δ , required

$$\Delta \approx 1/k_{\parallel\max} \approx d/\ln R \quad (13)$$

A scheme for subwavelength resolution was also proposed in (9) but, as noted above, this scheme depended on the existence of surface states derived from a mathematically postulated boundary for which no physical realization has so far been suggested.

Although our discussion has been in terms of electromagnetic waves, the same principles apply to any waves and particularly to acoustic waves, where time-reversal studies are also well developed (14).

Our original discussion (illustrated in Fig. 2) assumes a single-step transition from $+\omega$ to $-\omega$. Such processes occur but are very weak. At optical frequencies, perhaps the best system for the realization of these ideas is a four-wave mixing experiment: One of two counterpropagating pump beams of the same frequency as the signal writes a hologram. The second pump beam then reads the hologram to produce a time-reversed signal. In other words, there is a two-step process in which there first occurs a transition $+\omega \rightarrow 0$ and then a second transition $0 \rightarrow -\omega$. This process has much in common with the recent proposal for a subwavelength focusing device (15), except that in our scheme the system writes its own hologram.

As a generalization of the analogy, any positively refracting medium can have the sign of its refraction reversed by coating the surface with a phase-reversing sheet. This leads to the possibility of curved lenses that can magnify an object (16).

In principle, our new lens can be realized if the hologram is written in a thin sheet of nonlinear material. In practice, such a hologram would be very weak, and instead, 3D holograms are written if a strong output is desired. As a consequence of the 3D nature of the hologram, the second phase-reversed beam (shown on the right of Fig. 1C) is not seen, but if the left-hand surface of the medium is half silver (Fig. 4), reflection of the phase-reversed beam will generate an image

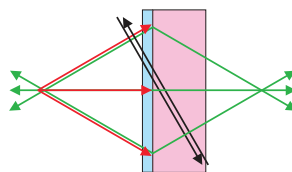


Fig. 4. In a four-wave mixing experiment, two counterpropagating waves first create a hologram and then diffract off the hologram to form a phase-reversed beam. A half-silvered mirror reflects the reversed beam to form an image on the far side of the system.

to the right of the system reproducing the effect predicted in Fig. 1C and mimicking the Veselago negatively refracting lens. However, the 3D nature of the hologram precludes any subwavelength resolution.

Creating a 2D hologram and attaining the ideal shown in Fig. 3 will be a challenge. Enhancing the nonlinearity of existing media—possibly through the use of plasmonic or metamaterial layers to enhance the local fields (17)—may offer a route to realizing a 2D version and hence subwavelength resolution. Further discussion of the practicalities of a four-wave mixing scheme can be found in the SOM.

References and Notes

1. J. P. Woerdman, *Opt. Commun.* **2**, 212 (1970).
2. P. Yeh, *Introduction to Photorefractive Nonlinear Optics* (Wiley, New York, 1993).

3. V. G. Veselago, *Sov. Phys. Usp.* **10**, 509 (1968).
4. J. B. Pendry, *Contemp. Phys.* **45**, 191 (2004).
5. J. B. Pendry, *Science* **306**, 1353 (2004).
6. K. Kobayashi, *J. Phys. Condens. Matter* **18**, 3703 (2006).
7. V. V. Cheianov, V. Fal'ko, B. L. Altshuler, *Science* **315**, 1252 (2007).
8. M. Nieto-Vesperinas, E. Wolf, *J. Opt. Soc. Am. A* **2**, 1429 (1985).
9. S. Maslovski, S. Tretyakov, *J. Appl. Phys.* **94**, 4241 (2003).
10. O. Malyuskin, V. Fusco, A. G. Schuchinsky, *IEEE Trans. Antenn. Propag.* **54**, 1399 (2006).
11. C. A. Allen, K. M. K. H. Leong, T. Itoh, *IEEE Int. Microwave Theory Tech. Symp. Dig.* **3**, 1875 (2003).
12. M. Wubs, A. Lagendijk, *Phys. Rev. E Stat. Nonlin. Soft Matter Phys.* **65**, 046612 (2002).
13. J. B. Pendry, *Phys. Rev. Lett.* **85**, 3966 (2000).
14. S. Yon, M. Tanter, M. Fink, *J. Acoust. Soc. Am.* **113**, 1533 (2003).
15. R. Merlin, *Science* **317**, 927 (2007); published online 11 July 2007 (10.1126/science.1143884).
16. J. B. Pendry, S. A. Ramakrishna, *J. Phys. Condens. Matter* **15**, 6345 (2003).
17. J. B. Pendry, A. J. Holden, D. J. Robbins, W. J. Stewart, *IEEE Trans. Microwave Theory Tech.* **47**, 2075 (1999).
18. I thank the Engineering and Physical Sciences Research Council for a Senior Fellowship, M. Damsen for educating me in various aspects of four-wave mixing, S. Maier for discussions on plasmonic enhancements of fields, and A. Lagendijk for comments on the manuscript.

Supporting Online Material

www.sciencemag.org/cgi/content/full/1162087/DC1
SOM Text
Figs. S1 to S6

20 June 2008; accepted 20 August 2008

Published online 28 August 2008;

10.1126/science.1162087

Include this information when citing this paper.

Surface-Modified Carbon Nanotubes Catalyze Oxidative Dehydrogenation of *n*-Butane

Jian Zhang, Xi Liu, Raoul Blume, Aihua Zhang, Robert Schlögl, Dang Sheng Su*

Butenes and butadiene, which are useful intermediates for the synthesis of polymers and other compounds, are synthesized traditionally by oxidative dehydrogenation (ODH) of *n*-butane over complex metal oxides. Such catalysts require high O_2 /butane ratios to maintain the activity, which leads to unwanted product oxidation. We show that carbon nanotubes with modified surface functionality efficiently catalyze the oxidative dehydrogenation of *n*-butane to butenes, especially butadiene. For low O_2 /butane ratios, a high selectivity to alkenes was achieved for periods as long as 100 hours. This process is mildly catalyzed by ketonic C=O groups and occurs via a combination of parallel and sequential oxidation steps. A small amount of phosphorus greatly improved the selectivity by suppressing the combustion of hydrocarbons.

Transition metal oxides have been widely used as catalysts for the conversion of butane to C_4 alkenes, important industrial precursors for producing synthetic rubbers, plastics, and a number of industrially important chemicals. Despite a great deal of research, alkene selectivity in the current butane-to-butadiene process is severely limited (1). One important reason is that the unsaturated products are much more readily oxidized to CO_2 than is the starting alkane. The chemical complexity of

polyvalent metal oxides, although found to be necessary for catalytic activity, impedes satisfactory selectivity through isolation of active sites (2–6). For this reason, the origin of the catalytic activity is debated, and there is as yet no generally accepted picture of the reaction mechanism (7, 8).

Carbon materials have been reported to catalyze the oxidative dehydrogenation (ODH) of an aromatic molecule, ethylbenzene. However, conventional carbons, in particular activated carbon, underwent unavoidable deactivations

due to coking or combustion (9–12). Recently, it was shown that only well-nanostructured carbons are stable and coke-free catalysts for styrene synthesis (12, 13). Activation of C–H bonds in the ethyl group is considered to be coordinated by the ketonic carbonyl (C=O) group. Ethylbenzene has an aromatic moiety that enables relatively facile activation. Here, we report on surface-modified carbon nanotubes (CNTs) as a high-performance catalyst for the ODH of the much less active butane. Relative to metal-based catalysts, CNTs displayed an enhanced selectivity to C₄ alkenes, especially butadiene.

We conducted the reaction at 400° or 450°C with an O₂/butane ratio of 2.0. The product mixture contained only 1-butene, 2-butene, butadiene, CO₂, CO, and residual reactants; the resulting carbon balance was 100 ± 3% (fig. S1A) (14). In a blank experiment without catalyst, the alkene yield was as low as 0.9%. Over pristine CNTs, 88.9% of the converted butane was burnt, yielding 1.6% alkenes (Fig. 1A). Considering the intensive stability of CNTs in O₂ (fig. S1B) (14), we conclude that the CO₂ during the reaction mainly originated from the oxidation of the hydrocarbon feedstock and not from

burning of the carbon catalysts. Neither washing CNTs in HCl solution nor loading with acidic nitro group could enhance the selectivity to alkene (fig. S2) (14).

We then functionalized surfaces of pristine CNTs with oxygen-containing groups by refluxing and oxidizing them in concentrated HNO₃ (15). With the resulting oCNTs as catalyst, we observed an improved yield of 6.7% alkenes. The alkene yield was further enhanced to 13.8% after the oCNTs catalyst was additionally modified by passivating defects with phosphorus [P-oCNTs, 0.5 ± 0.1 weight percent (wt %) P]. The increase in alkene selectivity is partially explained in Fig. 1B, which compares the catalytic performance of oCNTs and P-oCNTs for three individual reactions: (i) ODH of butane, (ii) ODH of 1-butene, and (iii) combustion of butadiene. The passivation apparently suppresses the activation and deep oxidation of the alkene substrates.

A survey of recent literature showed that the P-oCNTs catalyst is as selective as the best V/MgO catalyst developed during the past 20 years (fig. S3A) (14). To compare the present reaction conditions to those previously used, we synthesized and evaluated two V/MgO samples. At the same conversion of butane, the Mg₃V₂O₈ and Mg₃V₂O₇ samples were less selective than P-oCNTs (fig. S3B) (14); in particular, relative to Mg₃V₂O₇, P-oCNTs gave twice the selectivity to butadiene (16.2%).

Safety can be a challenge when mixing hydrocarbons with oxidants. One solution is to operate the reaction under anaerobic conditions. After we reduced the O₂/butane ratio from 2.0 to 0.5, the P-oCNTs sample still exhibited outstanding stability. During a reaction lasting 100 hours, the butane and oxygen conversion remained almost unchanged, and the alkene selectivity stayed above 53% (Fig. 1C). To the best of our knowledge, the oxidative stability of P-oCNTs far exceeds those of metal oxide catalysts, which only work well with excess oxygen (O₂/butane ≥ 2), a condition necessary to prevent severe deactivation due to coke deposition.

In Fig. 1D, we show the ODH activity of oCNTs and P-oCNTs as a function of residence time. These results demonstrate that the overall reaction comprises a combination of parallel and sequential oxidation steps. The alkene selectivity at zero residence time was not unity (16), indicating that direct butane combustion occurred in parallel with the ODH reactions (i.e., butane to butenes, butane to butadiene). Two reaction pathways to butadiene were identified. Selectivity toward butadiene remained finite at the zero residence time, evidencing a primary ODH of butane to butadiene; it increased with the residence time as the selectivity of butenes decreased, revealing a secondary ODH of butenes to butadiene.

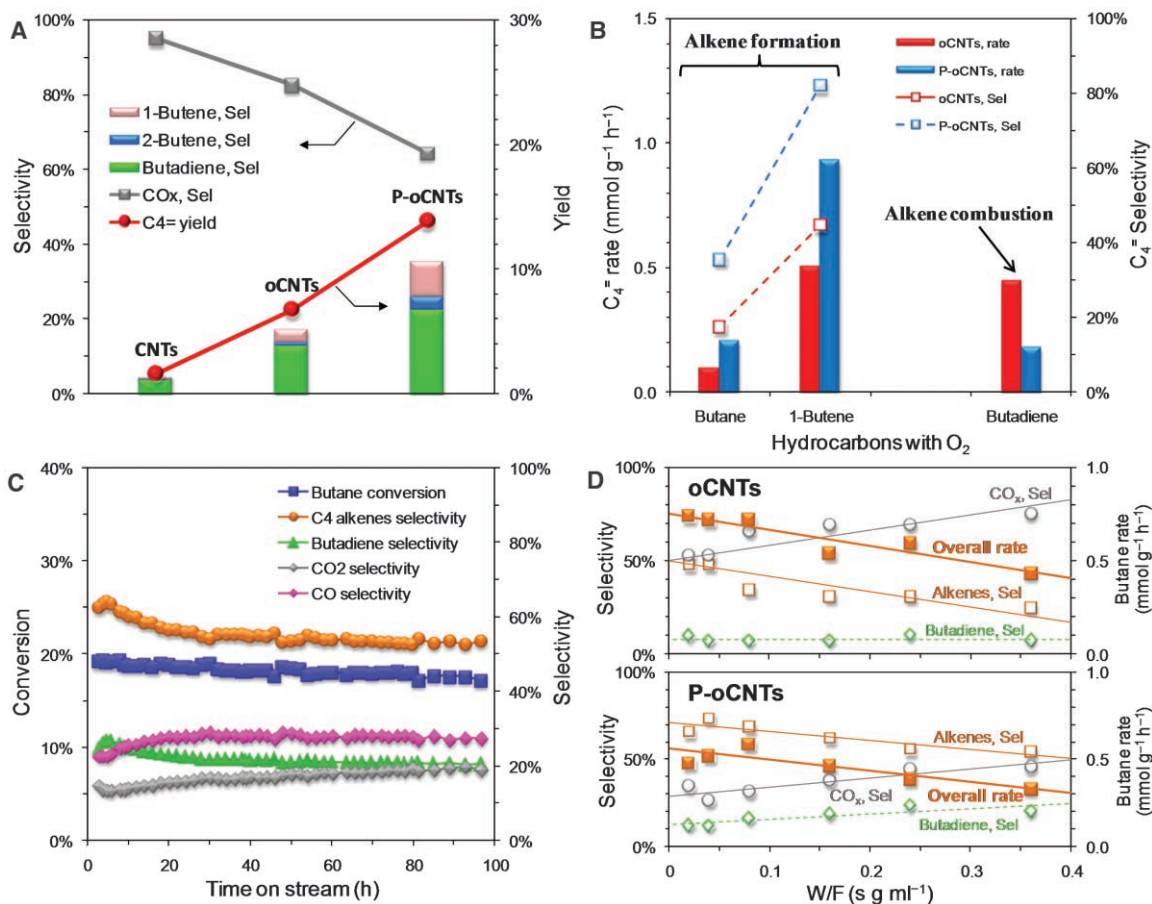
The effect of phosphorus as a promoter was studied by kinetic measurements. The initial rate

Fritz Haber Institute of the Max Planck Society, Faradayweg 4-6, D-14195 Berlin, Germany.

*To whom correspondence should be addressed. E-mail: dangsheng@fhi-berlin.mpg.de

Fig. 1. ODH activities of various carbon nanotubes.

(A) Performance of various CNTs for ODH of butane under oxygen-rich conditions: 0.18 g, 0.67% butane, O₂/butane = 2, 15 ml min⁻¹, 400°C. **(B)** Performance of modified CNTs in ODH reactions of butane and 1-butene and in combustion of butadiene: 0.18 g, 0.67% C₄ hydrocarbon, O₂/butane = 2, 15 ml min⁻¹, 400°C. **(C)** Stability of P-oCNTs catalyst for ODH of butane over 100 hours: 0.18 g, 2.7% butane, O₂/butane = 0.5, 10 ml min⁻¹, 450°C. **(D)** Dependence of product selectivity and reaction rate on residence time (W/F) in ODH reaction of butane: 0.005 to 0.09 g, 2.7% butane, O₂/butane = 0.5, 10 ml min⁻¹, 450°C. Helium was used as balance gas in all experiments.



constants for primary reactions were quantified as the residence time approached zero (16). After the modification with P, three important changes happened at the initial state: (i) The overall rate of converted butane decreased from 0.75 to 0.56 $\text{mmol g}^{-1} \text{hour}^{-1}$; (ii) the combustion of butane was reduced by as much as a factor of 2.3; and

(iii) the formation rate of alkenes kept nearly unchanged at 0.38 to 0.40 $\text{mmol g}^{-1} \text{hour}^{-1}$. Therefore, P increased the selectivity by suppressing the combustion rate, rather than enhancing the formation rate of alkenes.

One of the key concerns in identifying and describing metal-free catalysis is the suspected

influence of metal impurities in the catalyst. Commercial CNTs were prepared on supported metal catalysts, which inevitably remain as metal contaminants. Post-treatment by refluxing in strong acid effectively removed the residual metals to a great extent. X-ray fluorescence spectrometry revealed that the residual metals in the tested CNTs were very low (table S1) (14). The highest value of residual Fe was still as low as 0.09 wt %, as confirmed by energy-dispersive x-ray analysis (around 0.1 wt %). Furthermore, there was no signal of Fe or other metals in the surface layer at the limit of detection by synchrotron-excited x-ray photoelectron spectroscopy (XPS) (Fig. 2A). This difference suggests that if there is residual metal, it must be embedded in the carbon and not exposed to the reactants. This explanation is supported by the high-resolution transmission electron microscopy (HRTEM) image in Fig. 2B, which shows a catalyst particle encapsulated inside the CNTs. To fully exclude the role of Fe in the reaction, we deliberately added Fe to oCNTs in fractions ranging from 0.05 to 0.5 wt %. As shown in Fig. 2C, both the butane conversion and selectivity to C_4 alkenes gradually decreased with the increasing Fe content. Furthermore, there was no correlation of alkene selectivity with the residual metal content (fig. S4A) (14). We prepared a sample with 5% Fe phosphate in oCNTs; this sample also exhibited performance inferior to that of P-oCNTs without Fe (fig. S4B) (14). We can thus conclude that the reactivity originated exclusively from metal-free active sites on CNTs and that the residual metals played no positive role.

To elucidate the structure-activity relation, we studied the morphological features by TEM with elemental mapping. Figure 3A gives an overview elemental map from a typical area. Both P and O are dispersed throughout the sample without aggregation. After an ODH reaction that ran for more than 800 min, the morphology of the CNTs remained intact and no evidence for their combustion was identified (Fig. 3B), as expected from the thermal stability data (fig. S1B) (14). Some areas of the outer and inner walls of the CNTs were covered by thin layers of phosphorus, which obviously differs from fullerene carbon species on pristine CNTs originating from condensation of hydrocarbon fragments (fig. S5) (14). Most of the surface of the CNTs did not give rise to carbon deposition, which is one advantage of this metal-free catalyst.

We also monitored the working surface of CNTs with near-ambient XPS (17). The best P-oCNTs catalyst was heated in vacuum to 350°C; at this temperature, the less stable groups (anhydride, carboxyl, ester, and nitro) would already have desorbed from the surface (fig. S6) (14). We identified two contributions from ketonic C=O groups ($531.2 \pm 0.2 \text{ eV}$) and from C-O groups ($533.1 \pm 0.2 \text{ eV}$) (i.e., ether and hydroxyl) (15, 18). Relative amounts of C-O and C=O are represented in Fig. 3C by the ratio

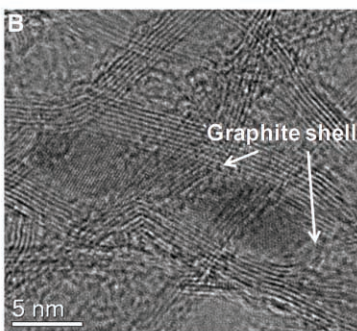
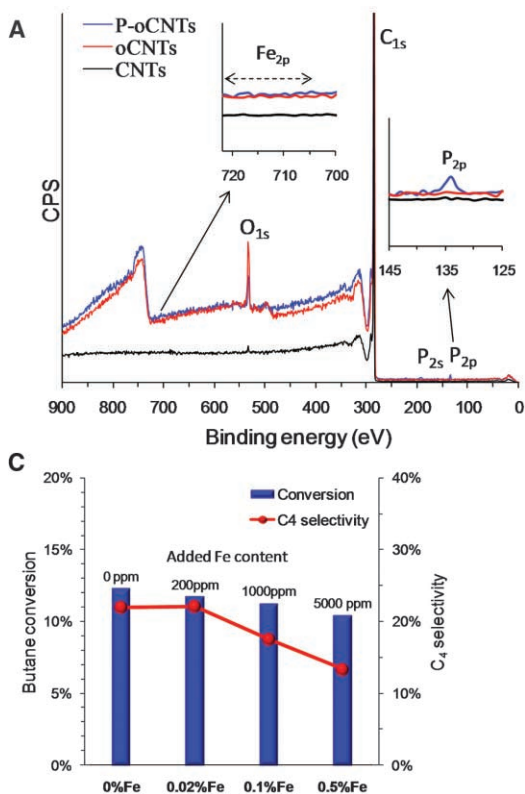


Fig. 2. (A) Synchrotron-excited XPS spectra of CNT samples. (B) HRTEM image of residual metal particles encapsulated inside CNTs. (C) Effect of added Fe on the activity of oCNTs: 0.18 g, 2.7% butane, $\text{O}_2/\text{butane} = 0.5$, 10 ml min^{-1} , 450°C. Helium was used as balance gas.

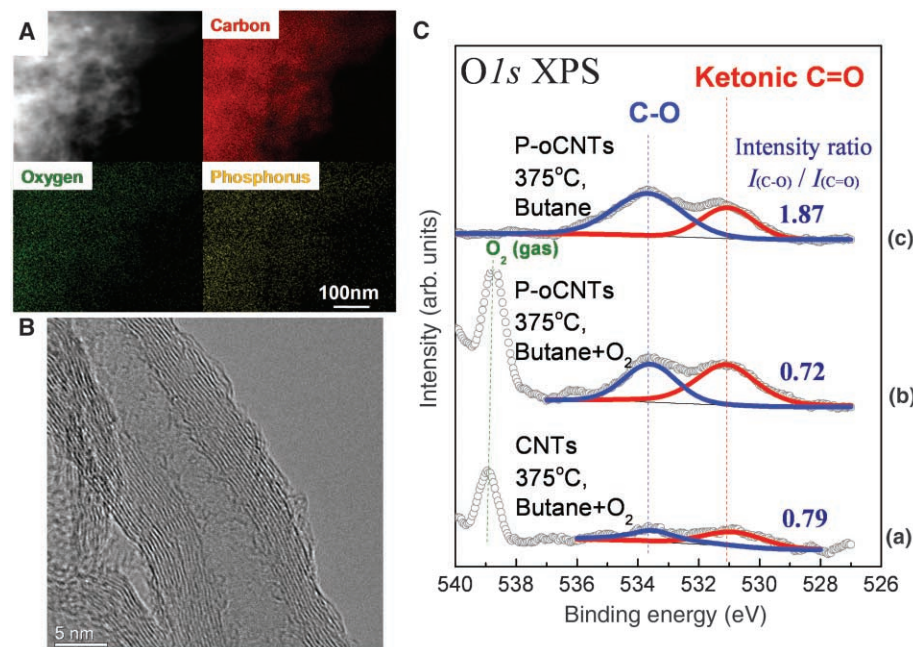


Fig. 3. (A) Elemental maps and (B) HRTEM image of the used P-oCNTs in Fig. 1A. (C) In situ $\text{O}1s$ XPS spectra of working catalysts taken at 350° to 375°C: (a) CNTs: butane + O_2 (1:1), 0.25 mbar; (b) P-oCNTs: butane + O_2 (1:1), 0.25 mbar; (c) P-oCNTs: butane, 0.125 mbar.

of their intensities, $I_{C=O}/I_{C-O}$. Under ODH conditions (butane + O₂, 1:1, 0.25 atm, 350° to 375°C), $I_{C=O}/I_{C-O}$ values ranged from 0.72 to 0.80. However, after switching off O₂, the $I_{C=O}/I_{C-O}$ value sharply increased to 1.87 (Fig. 3C) and the activity went to almost zero. This finding indicates that ketonic C=O groups are a critical ingredient of the active sites, whereas C–O groups constitute inactive intermediates or adsorbates.

Figure 4A summarizes our proposed mechanism for the CNTs-catalyzed butane oxidation. For this purpose, surface oxygen species are classified into electrophilic (superoxide O₂^{•−}, peroxide O₂^{2−}) and nucleophilic (O^{2−}) types (19). Electrophilic oxygen species are electron-deficient and attack the electron-rich C=C bonds in alkenes, leading to the rupture of the carbon skeleton and subsequent combustion. Pristine CNTs were produced from chemical vapor deposition of unsaturated hydrocarbons, resulting in a number of structural defects and terminal carbon fragments. Below 600°C, these defect sites or edges of graphene have been reported to convert O₂ molecules to electrophilic oxygen species (20) and thus cause low selectivity to alkenes.

More controlled oxidation of carbon surfaces can be carried out in liquid-phase oxidants (21).

After refluxing in HNO₃, defect sites were functionalized by O^{2−} anions into various functional groups. For example, ketonic C=O, a nucleophilic species with high electron density, preferentially reacts with electron-poor saturated bonds. However, at the reaction temperature, desorption of less stable groups results in new graphitic defects that subsequently generate new electrophilic oxygen sites, thus partially limiting the selectivity to alkenes on oCNTs. The addition of phosphate reacting with these defects suppresses the formation of electrophilic oxygen species (22). Thus, P-oCNTs displayed a lower overall activity but a much better selectivity.

We used density functional theory (DFT) calculations with the CASTEP code and the Perdew-Burke-Ernzerhof generalized gradient approximation (23, 24) to study the ODH reaction over ketonic C=O groups. These calculations are independent of the precise mechanism and the transition state of each elementary step. We used the graphitic zigzag edge as a model to anchor the ketonic C=O groups (Fig. 4B). Conversion of butane is energetically controlled by the abstraction of the first H atom, which was predicted to be mildly endothermic at 0.92 eV. To convert butane into 1- or 2-butene,

two C=O sites would ultimately be needed, and each one returns a single electron to the surrounding graphene as the reservoir. The remaining H atoms combine with surrounding oxygen to water, thereby closing the primary ODH cycle. The enthalpy of formation of water compensates for the endothermic dehydrogenation of butane. As a consequence, the calculated free energies for formation of 1- and 2-butenes were −0.88 eV and −1.03 eV, respectively. Another pathway to regenerate active sites is that H atoms recombine into H₂ molecules. However, as expected, such a direct dehydrogenation reaction is energetically unfavorable, because energy barriers are as high as 1.45 to 1.60 eV.

The DFT calculation also provides insights into the reaction pathways to butadiene. Butadiene may directly form from butane as primary product with an overall energy of −1.97 eV. However, the need for neighboring C=O sites to accommodate four H atoms in one elementary step does not seem to be pronounced, accounting for a much lower rate than the secondary ODH from butenes (Fig. 1D). It is more likely that C=O primarily activates butenes (rather than butane) to butadiene. The energy for the abstraction of the first H from butenes ($\Delta E_{\text{butenes,1H}}$), 0.25 to 0.40 eV, is much lower than that from butane ($\Delta E_{\text{butane,1H}}$), 0.92 eV. In this way, we can understand the influence of residence time. Because the residence time is long enough for the butenes produced to diffuse and react with the surrounding C=O sites, butadiene will be primarily generated from the secondary ODH, as demonstrated by the prevailing fraction of butadiene in C₄ alkenes in an integral reaction, 63 to 74% (Fig. 1A).

Our work contains some implications for catalysis in general. It is possible to imitate heterogeneously the concepts of homogeneous metal-free catalysis. The function of oxygen heteroatoms in molecular catalysts is reproduced by defects of bent graphitic sheets. The catalytic principle of site isolation can be realized by electronic localization of charges at the defect sites corresponding to molecular analogs of double bonds. The operation mode of ODH reactions can be studied on metal-free catalysts with greater precision than in metal oxide systems. There is neither lattice nor structural oxygen, but only oxygen at active sites. The present catalysts are free of polyvalent metal sites with complex electronic and spin structures, allowing for a facile theoretical treatment. Finally, the application of a heterogeneous CNTs catalyst is attractive because of favorable management of energy over a good thermal and electronic conductor.

References and Notes

1. F. Cavani, F. Trifirò, *Appl. Catal. A* **133**, 219 (1995).
2. R. Grabowski, *Catal. Rev.* **48**, 199 (2006).
3. K. D. Chen, A. T. Bell, E. Iglesia, *J. Catal.* **209**, 35 (2002).
4. G. I. Panov, K. A. Dubkov, E. V. Starokon, *Catal. Today* **117**, 148 (2006).
5. A. Miyakoshi, A. Ueno, M. Ichikawa, *Appl. Catal. A* **219**, 249 (2001).
6. L. B.-Tapia, I. H. Pérez, P. Schacht, I. R. Córdova, G. G. Aguilar-Ríos, *J. Catal.* **107–108**, 371 (2005).
7. E. V. Kondratenko, M. Cherian, M. Baerns, *Catal. Today* **99**, 59 (2005).

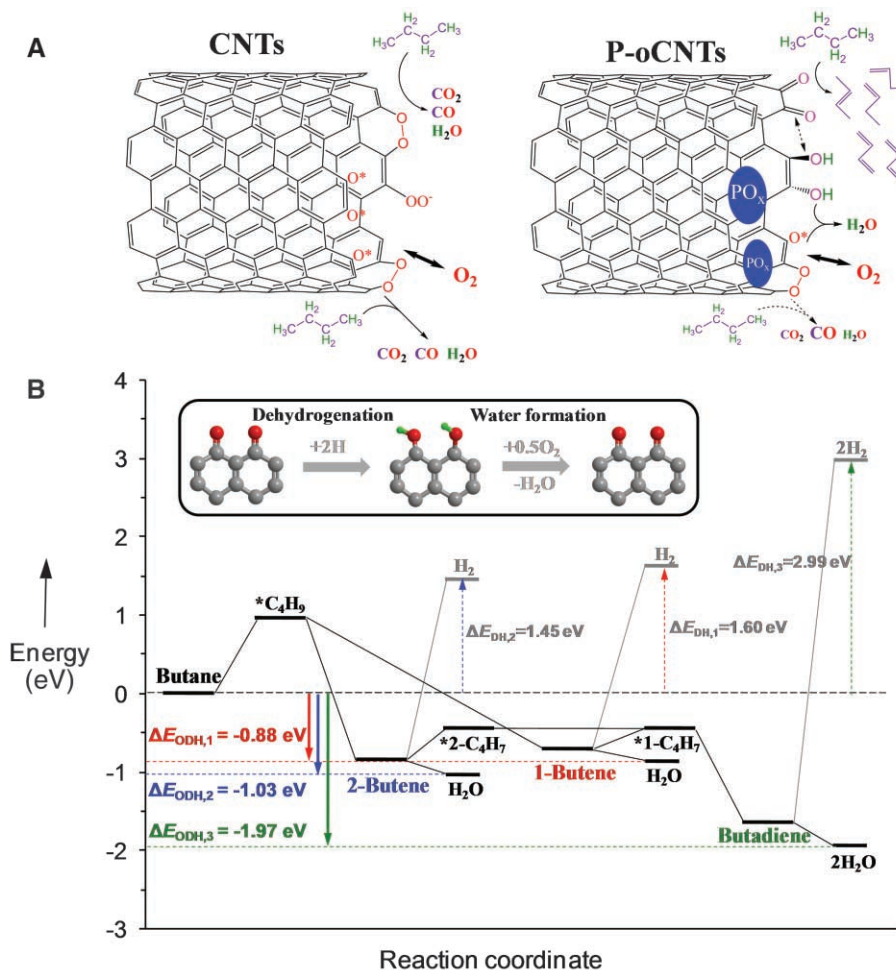


Fig. 4. (A) Schematic reaction and (B) energy steps of butane oxidation on pristine and P-modified CNTs.

- C. Resini, T. Montanari, G. Busca, J.-M. Jehng, I. E. Wachs, *Catal. Today* **99**, 105 (2005).
- T. G. Alkhozov, E. A. Ismailov, A. Yu, A. I. Kozharov, *Kinet. Katal.* **19**, 611 (1978).
- M. S. Kane, L. C. Kao, R. K. Mariwala, D. F. Hilscher, H. C. Foley, *Ind. Eng. Chem. Res.* **35**, 3319 (1996).
- M. F. R. Pereira, J. J. M. Órfão, J. L. Figueiredo, *Appl. Catal. A* **218**, 307 (2001).
- J. Zhang *et al.*, *Angew. Chem. Int. Ed.* **46**, 7319 (2007).
- G. Mestl, N. I. Maksimova, N. Keller, V. V. Roddatis, R. Schlögl, *Angew. Chem. Int. Ed.* **40**, 2066 (2001).
- See supporting material on Science Online.
- J.-H. Zhou *et al.*, *Carbon* **9**, 1379 (2007).
- K. D. Chen, E. Iglesia, A. T. Bell, *J. Phys. Chem. B* **105**, 646 (2001).
- M. Salmeron, R. Schlögl, *Surf. Sci. Rep.* **63**, 169 (2008).
- T. I. T. Okpalugo, P. Papakonstantinou, H. Murphy, J. McLaughlin, N. M. D. Brown, *Carbon* **43**, 153 (2005).
- L. M. Madeira, M. F. Portela, *Catal. Rev.* **44**, 247 (2002).
- F. Atamny *et al.*, *Mol. Phys.* **76**, 851 (1992).
- M. L. Toebe, J. M. P. van Heeswijk, J. H. Bitter, A. J. van Dillen, K. P. de Jong, *Carbon* **42**, 307 (2004).
- A. M. Puziy, O. I. Poddubnaya, A. M. Ziatdinov, *Appl. Surf. Sci.* **252**, 8036 (2006).
- S. J. Clark *et al.*, *Z. Kristallogr.* **220**, 567 (2005).
- J. P. Perdew, K. Burke, M. Ernzerhof, *Phys. Rev. Lett.* **77**, 3865 (1996).
- We thank the Max Planck Society; U. Wild, A. Klein-Hoffmann, and J. Thielemann for technical assistance; Berliner Elektronenspeicherring-Gesellschaft

für Synchrotronstrahlung for support of in situ XPS measurements; and M. A. Smith for helpful discussions. Supported by the CANAPE project of the 6th Framework Programme of European Commission and the ENERChem project of the Max Planck Society.

Supporting Online Material

www.sciencemag.org/cgi/content/full/322/5898/73/DC1

Materials and Methods

Figs. S1 to S6

Table S1

References

17 June 2008; accepted 21 August 2008

10.1126/science.1161916

Merging Photoredox Catalysis with Organocatalysis: The Direct Asymmetric Alkylation of Aldehydes

David A. Nicewicz and David W. C. MacMillan*

Photoredox catalysis and organocatalysis represent two powerful fields of molecule activation that have found widespread application in the areas of inorganic and organic chemistry, respectively. We merged these two catalysis fields to solve problems in asymmetric chemical synthesis. Specifically, the enantioselective intermolecular α -alkylation of aldehydes has been accomplished using an interwoven activation pathway that combines both the photoredox catalyst $\text{Ru}(\text{bpy})_3\text{Cl}_2$ (where bpy is 2,2'-bipyridine) and an imidazolidinone organocatalyst. This broadly applicable, yet previously elusive, alkylation reaction is now highly enantioselective and operationally trivial.

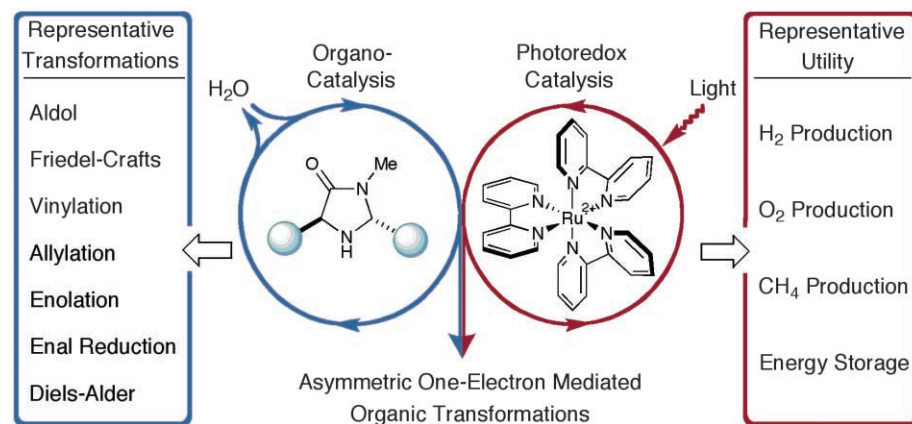
Nature's ability to convert solar energy to chemical energy in photosynthesis has inspired the development of a host of photoredox systems in efforts to mimic this process. Arguably the most studied one-electron photoredox catalyst has been $\text{Ru}(\text{bpy})_3^{2+}$ (where bpy is 2,2'-bipyridine): an inorganic complex that has facilitated important advances in the areas of energy storage, hydrogen and oxygen evolution from water, and methane production from carbon dioxide (1, 2). Given its proven ability to mediate electron transfer, it is surprising that $\text{Ru}(\text{bpy})_3^{2+}$ has not found a substantial application in organic synthesis, wherein a large number of fundamental reactions rely on the generation and exploitation of radicals or single-electron intermediates (3).

Over the past decade, the field of organocatalysis has grown at a dramatic pace, providing more than 130 chemical reactions that rapidly facilitate enantioselective C–C, C–O, C–N, and C–halogen bond formation (4, 5). Whereas a broad range of reaction types have recently succumbed to this mode of catalysis (including aldol, Friedel–Crafts, and cycloadditions), it is important to consider that nearly all organocatalytic bond constructions are restricted to two-electron pathways, wherein the highest occupied molecular

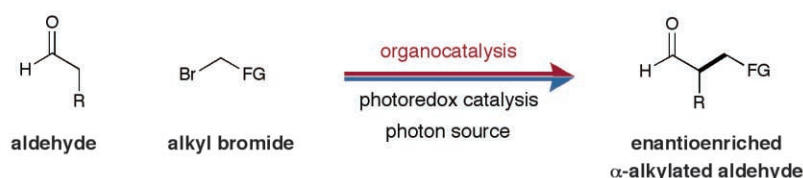
orbital of an electron-rich substrate reacts with the lowest unoccupied molecular orbital of an electron-deficient partner. Recently, however, our

laboratory introduced the concept of organo-singly occupied molecular orbital (SOMO) catalysis, a one-electron mode of activation that has enabled the development of several useful transformations (6–10).

Given the widespread success of both electron transfer catalysis and organocatalysis, we recently questioned whether it might be possible to merge these two powerful areas, with the goal of solving long-standing, yet elusive problems in chemical synthesis. More specifically, as a blueprint for reaction invention, we hoped to exploit the lessons of photoredox enzymatic catalysis (11), wherein a series of consecutive low-barrier, open-shell steps are energetically preferred to high-barrier, two-electron pathways. On this basis, we hypothesized that the enantioselective catalytic α -alkylation of aldehydes (12–15), a widely sought yet elusive transformation, might be brought to fruition via the marriage of inorganic electron transfer and organic catalysis (Fig. 1).



Enantioselective Catalytic Carbonyl α -Alkylation



Contribution from Merck Center for Catalysis, Department of Chemistry, Princeton University, Princeton, NJ 08544, USA.

*To whom correspondence should be addressed. E-mail: dmacmill@princeton.edu

Fig. 1. Merging amine catalysis and organometallic photoredox catalysis to enable asymmetric organic transformations. Me, methyl; R, generic organic substituent; FG, electron-withdrawing functional group.